

1 **COVIDpro: Database for mining protein dysregulation in patients with COVID-19**

2

3 Fangfei Zhang^{1,2,3,4}, Augustin Luna⁵, Tingting Tan^{1,2,3,4}, Yingdan Chen⁶, Chris Sander⁷,
4 Tiannan Guo^{1,2,3*}

5

6 ¹Westlake Laboratory of Life Sciences and Biomedicine, Key Laboratory of Structural
7 Biology of Zhejiang Province, School of Life Sciences, Westlake University, Hangzhou,
8 Zhejiang Province, China

9 ²Institute of Basic Medical Sciences, Westlake Institute for Advanced Study, Hangzhou,
10 Zhejiang Province, China

11 ³Research Center for Industries of the Future, Westlake University, 600 Dunyu Road,
12 Hangzhou, Zhejiang, 310030, China

13 ⁴Center for Infectious Disease Research, Westlake University, 18 Shilongshan Road,
14 Hangzhou 310024, Zhejiang, China

15 ⁵Department of Data Sciences, Dana-Farber Cancer Institute, Boston, MA

16 ⁶Westlake Omics (Hangzhou) Biotechnology Co., Ltd., Hangzhou, Zhejiang Province, China

17 ⁷Systems Biology, Harvard Medical School, Boston, MA

18 **Summary**

19

20 **Background**

21 The ongoing pandemic of the coronavirus disease 2019 (COVID-19) caused by the severe
22 acute respiratory syndrome coronavirus 2 (SARS-CoV-2) still has limited treatment options
23 partially due to our incomplete understanding of the molecular dysregulations of the COVID-
24 19 patients. We aimed to generate a repository and data analysis tools to examine the
25 modulated proteins underlying COVID-19 patients for the discovery of potential therapeutic
26 targets and diagnostic biomarkers.

27

28 **Methods**

29 We built a web server containing proteomic expression data from COVID-19 patients with a
30 toolset for user-friendly data analysis and visualization. The web resource covers expert-
31 curated proteomic data from COVID-19 patients published before May 2022. The data were
32 collected from ProteomeXchange and from select publications via PubMed searches and
33 aggregated into a comprehensive dataset. Protein expression by disease subgroups across
34 projects was compared by examining differentially expressed proteins. We also visualize
35 differentially expressed pathways and proteins. Moreover, circulating proteins that
36 differentiated severe cases were nominated as predictive biomarkers.

37

38 **Findings**

39 We built and maintain a web server COVIDpro (<https://www.guomics.com/covidPro/>)
40 containing proteomics data generated by 41 original studies from 32 hospitals worldwide,
41 with data from 3077 patients covering 19 types of clinical specimens, the majority from
42 plasma and sera. 53 protein expression matrices were collected, for a total of 5434 samples
43 and 14,403 unique proteins. Our analyses showed that the lipopolysaccharide-binding protein,
44 as identified in the majority of the studies, was highly expressed in the blood samples of
45 patients with severe disease. A panel of significantly dysregulated proteins was identified to
46 separate patients with severe disease from non-severe disease. Classification of severe disease
47 based on these proteomic signatures on five test sets reached a mean AUC of 0.87 and ACC
48 of 0.80.

49

50 **Interpretation**

51 COVIDpro is an online database with an integrated analysis toolkit. It is a unique and
52 valuable resource for testing hypotheses and identifying proteins or pathways that could be
53 targeted by new treatments of COVID-19 patients.

54

55 **Funding**

56 National Key R&D Program of China: Key PDPM technologies (2021YFA1301602,
57 2021YFA1301601, 2021YFA1301603), Zhejiang Provincial Natural Science Foundation for
58 Distinguished Young Scholars (LR19C050001), Hangzhou Agriculture and Society
59 Advancement Program (20190101A04), National Natural Science Foundation of China
60 (81972492) and National Science Fund for Young Scholars (21904107), National Resource
61 for Network Biology (NRNB) from the National Institute of General Medical Sciences
62 (NIGMS -P41 GM103504)

63 **Research in context**

64 **Evidence before this study**

65 Although an increasing number of therapies against COVID-19 are being developed, they are
66 still insufficient, especially with the rise of new variants of concern. This is partially due to
67 our incomplete understanding of the disease's mechanisms. As data have been collected
68 worldwide, several questions are now worth addressing via meta-analyses. Most COVID-19
69 drugs function by targeting or affecting proteins. Effectiveness and resistance to therapeutics
70 can be effectively assessed via protein measurements. Empowered by mass spectrometry-
71 based proteomics, protein expression has been characterized in a variety of patient specimens,
72 including body fluids (e.g., serum, plasma, urea) and tissue (i.e., formalin-fixed and paraffin-
73 embedded (FFPE)). We expert-curated proteomic expression data from COVID-19 patients
74 published before May 2022, from the largest proteomic data repository ProteomeXchange as
75 well as from literature search engines. Using this resource, a COVID-19 proteome meta-
76 analysis could provide useful insights into the mechanisms of the disease and identify new
77 potential drug targets.

78

79 **Added value of this study**

80 We integrated many published datasets from patients with COVID-19 from 11 nations, with
81 over 3000 patients and more than 5434 proteome measurements. We collected these datasets
82 in an online database, and generated a toolbox to easily explore, analyze, and visualize the
83 data. Next, we used the database and its associated toolbox to identify new proteins of
84 diagnostic and therapeutic value for COVID-19 treatment. In particular, we identified a set of
85 significantly dysregulated proteins for distinguishing severe from non-severe patients using
86 serum samples.

87

88 **Implications of all the available evidence**

89 COVIDpro will support the navigation and analysis of patterns of dysregulated proteins in
90 various COVID-19 clinical specimens for identification and verification of protein
91 biomarkers and potential therapeutic targets.

92 **Introduction**

93 Since the end of 2019, the world population has been threatened by the severe acute
94 respiratory syndrome coronavirus 2 (SARS2-CoV-2) and the ongoing rise of its constantly
95 evolving variants that have the potential for increased transmissibility, morbidity, and
96 mortality¹. The spread of coronavirus disease 2019 (COVID-19) shows no signs of being
97 restrained, and drugs with new daily cases worldwide regularly surpassing 1 million². Drugs
98 to treat SARS2-CoV-2 are still insufficiently effective^{3,4}.

99
100 Most COVID-19 drugs, if not all, target or act through proteins. Specifically, they mainly
101 target the RNA-dependent RNA polymerase (RdRp) and the main protease of the virus
102 (3CLpro or Mpro), thus inhibiting virus entry and replication^{5,6}. However, most of the
103 targeted proteins are not human, partially due to the limited understanding of the molecular
104 dysregulation occurring in patient specimens⁷. Furthermore, proteins are not only relevant as
105 drug targets: they can be robust diagnostic and prognostic biomarkers and the effectiveness of
106 certain drugs can be better assessed via protein measurements.

107
108 Using mass spectrometry (MS)-based proteomics, the expression of thousands of proteins can
109 be simultaneously profiled in a variety of patient specimens, including body fluids (e.g.,
110 serum, plasma, urine) and tissue (i.e., frozen or formalin-fixed paraffin-embedded (FFPE)).
111 Proteome studies have successfully identified novel biomarkers and drug targets in several
112 clinical studies⁸. Since the first molecular characterization of COVID-19 patient sera⁹, more
113 clinical specimens have been analyzed using mass spectrometry-based proteomics^{8,10}.
114 Proteomics data analysis offers unique insights for discovering new potential drug targets.
115 While most published studies analyzed in this research area have focused on the following
116 specimen types: blood samples, including serum¹¹⁻²¹, plasma^{12,13,22-32}, and peripheral blood
117 mononuclear cells (PBMC)^{33,34}, there are also studies analyzing FFPE tissue^{35,36}, urine³⁷⁻⁴¹,
118 fecal⁴², sputum²³, extracellular vesicle^{43,44}, cerebrospinal fluid²¹, semen⁴⁵, colostrum⁴⁶,
119 colostrum⁴⁷ and nasopharynx swabs samples⁴⁸. All these studies have provided proteomic
120 snapshots of different aspects of tissues from COVID-19 patients. However, few studies have
121 compared the results of multiple studies to fully evaluate this disease due to the lack of proper
122 software tools and databases. While other types of COVID-19 molecular databases exist⁴⁹⁻⁵²,
123 none of these is focused on proteomic data from patient samples.

124
125 In our meta-analysis, we expert-curated a selection of protein expression datasets published
126 until May 2022, as well as metadata related to the patient and sample information from over
127 3000 patients. We analyzed the differentially expressed proteins and pathways in various
128 conditions and identified patterns of recurrently altered protein expression, which can serve as
129 new potential drug targets for treating patients with COVID-19. We also generated a machine
130 learning model for stratifying COVID-19 severity.

132 **Methods**

133 **Literature search strategy and selection criteria**

134 To produce a comprehensive proteomics data of COVID-19 patients, we used two curation
135 approaches. First, we searched the literature in PubMed using the keywords ‘COVID-19’,
136 ‘patient’, ‘proteomics’, and ‘clinic’. Second, we searched ProteomeXchange, the largest
137 proteomics data repository, using the identifier ‘COVID-19’. Next, we manually went
138 through each study and collected data from their supplementary files. Using these data
139 collation procedures, we thus identified and collected data from 41 studies containing protein
140 expression datasets of COVID-19 patients.

141

142 The datasets were organized into tables with patient and sample information, together with
143 the protein expression data. The patient information table includes gender, age, and severity
144 of COVID-19, if available in the original studies. The sample information table describes the
145 types of clinical specimen, the sample preparation, and the methods used for the proteomics
146 data acquisition. For studies using more than two types of clinical specimens, we divided the
147 sample information of each type into separate datasets to facilitate meta-analytic comparisons.
148 The protein expressions were then represented as the measured signals of each protein in each
149 sample. Since protein group quantifications can be ambiguous, we included unique proteins.

150

151 **Data analysis**

152 **Patient, sample, and data information**

153 When stratifying patients for analysis, we focused on the information that most studies
154 provide about patients: gender, age, and disease subgroup. The disease subgroups describe
155 each patient's severity level by symptoms. We included the following subgroups: healthy
156 donors, non-COVID-19 controls, COVID-19 (non-severe), COVID-19 (severe), COVID-19
157 (critical), COVID-19 (non-critical) and COVID-19 (fatal) patients. Disease severity was
158 determined using World Health Organization scores¹⁶. For several studies, we further
159 classified patients according to their diagnosis of pulmonary fibrosis or their levels of
160 interleukin-6 (IL-6). The datasets were derived from 12 types of clinical specimens: plasma,
161 serum, urine, peripheral blood mononuclear (PBMC), bronchoalveolar lavage fluid,
162 colostrum, extracellular vesicle (EV), feces, nasopharynx swabs, sputa, and FFPE samples
163 derived from heart, kidney, liver, lung, spleen, testis, and thyroid. The sample preparation
164 methods included serum depletion, serum non-depletion, plasma depletion, plasma non-
165 depletion, breast pump, fecal boiling, filter 3kDa, iST kit, methanol precipitation, immune
166 affinity purification, dithiothreitol, ethanol precipitation, acetone precipitation, pressure
167 cycling technology (PCT), RapiGest, red blood cell (RBC) removal, sonication,
168 ultracentrifugation, and others. The proteomics data acquisition methods included data-
169 dependent acquisition (DDA), tandem-mass tags (TMT), enzyme-linked immunosorbent
170 assay (ELISA), multiple reaction monitoring (MRM), data-independent acquisition (DIA),
171 sequential window acquisition of all theoretical fragment ion spectra (SWATH), scanning
172 SWATH (sSWATH), and O-link assays. The proteins included in the database are identified
173 by their UniProt names or HUGO Gene Nomenclature Committee gene names.

174

175 **Detection of proteins in different datasets and functional roles**

176 Proteins that were identified in multiple datasets were used for further exploration. We list
177 the fraction of missed detection by mass spectrometry for each protein in each dataset,
178 computed as the percentage of missed detections across all sample files in that dataset. Next,
179 we focused on the 76 proteins that were identified in more than 70% of datasets. The number
180 of unique proteins in the datasets are also listed. The proteins that were consistently identified
181 were analyzed using gene set enrichment analysis using GO, the R databases org.Hs.eg.db⁵³,
182 and the package clusterProfiler⁵⁴ for biological process analysis.

183

184 **Boxplot analysis of selected proteins**

185 The distributions of the protein abundances were organized by disease subgroups.
186 Specifically, we used grouped boxplots for each dataset and the R package ggboxplot.
187 Unpaired two-sided t-tests were performed with *p*-values calculated by comparing subgroup
188 pairs with the function of `t_test` in the R package rstatix with a normal distribution
189 assumption. The significance levels of the differential changes were indicated by the
190 corrected *p*-value of 0.5, 0.1, 0.01, and 0.001. For the dataset of Nie *et al.*, the protein
191 expression fold changes were calculated for different tissue types. For Tang *et al.*, Fisher *et*

192 *al.*, Lam *et al.*, and Zhong *et al.*, which contained information on the disease course, we
193 provided the temporal grouped boxplots with the loess smooth curve fitting regions. For the
194 D'Alessandro *et al.* dataset, the comparative groups were based on the levels of IL-6.

195

196 **Pathway analysis of differentially expressed proteins**

197 The molecular pathways containing proteins detected by a specific dataset can be visualized
198 using network graphs and the R package *cyjShiny*⁵⁵. A pair of disease subgroups can be
199 chosen so that the node size is proportional to the protein expression fold change; the fold
200 change is calculated as the ratio between the mean expression values in each group with an
201 unpaired two-sided t-test. Colors highlight only the nodes with significant changes. The
202 significantly dysregulated proteins were those with a p -value < 0.05 . KEGG and GO gene set
203 enrichment analyses were performed for such dysregulated proteins using the R package
204 *clusterProfiler*.

205

206 **Co-regulated differentially expressed proteins**

207 Given any two disease subgroups, we identified the proteins that were differentially
208 expressed in the same direction. Fold changes were calculated as the ratios of the mean
209 expression values, the p -values were calculated using an unpaired two-sided t-test between
210 the two chosen disease subtypes. The differentially expressed proteins were identified by the
211 user's cutoff fold change and p -value. Using a set of sera samples as an example, we
212 identified the proteins that were either up- or down-regulated (adjusted p -value < 0.05) in
213 more than five datasets in patients with severe disease vs. patients with non-severe diseases.
214 51 differentially expressed proteins were used to build a preliminary random forest model to
215 classify COVID-19 severity using the *Shen_1* data set as the training set. The resulting top
216 nine proteins were used to build a random forest-based classifier validated in five
217 independent datasets.

218

219 **Statistical packages**

220 The statistical analyses of this study used several R packages. Their names and associated
221 version numbers are: *org.Hs.eg.db* 3.12.0, *AnnotationDbi* 1.52.0, *IRanges* 2.24.1, *S4Vectors*
222 0.28.1, *Biobase* 2.50.0, *clusterProfiler* 3.18.1, *cyjShiny* 1.0.19, *base64enc* 0.1-3, *graph* 1.68.0,
223 *BiocGenerics* 0.36.1, *ggbeeswarm* 0.6.0, *pheatmap* 1.0.12, *rstatix* 0.7.0, *ggpubr* 0.4.0,
224 *ECharts2Shiny* 0.2.13, *jsonlite* 1.7.2, *igraph* 1.2.6, *htmlwidgets* 1.5.3, *leaflet* 2.0.4.1, *shiny*
225 1.6.0, *shinydashboard* 0.7.1, *DT* 0.18, *plotly* 4.9.4.1, *ggplot2* 3.3.5, *shinyWidgets* 0.6.0,
226 *shinythemes* 1.2.0, *RColorBrewer* 1.1-2, and *BiocManager* 1.30.16.

227

228 **Role of the funding source**

229 The study's funders were not involved in the study design, data collection, data analysis, data
230 interpretation, or report writing.

231

232 **Results**

233 A preliminary set of 41 studies was identified after systematic collection of proteomic data
234 for COVID-19 patients from a set of 316 search results collected from publications as the
235 result of PubMed searches and 178 collected from ProteomeXchange. After manually
236 scrutinizing the full-text and supplementary files of these studies, we selected those
237 containing patient proteomics data for further meta-analyses. The selected studies were
238 further grouped according to their clinical sample type. If a study contained multiple clinical
239 sample types, each sample type was considered a different project with a different dataset. As
240 a result, we collected 53 datasets involving samples from 3,077 patients, 5434 clinical
241 specimens, and 14,403 unique proteins (Figure 1A). For ease of presentation, the projects are

242 represented by author names and a numeric index. We uploaded all 53 datasets to a freely
243 accessible database: COVIDpro (<https://www.guomics.com/covidPro/>). Using this database,
244 users may select their projects of interest and query for perturbed proteins from specific
245 COVID-19 specimen types. For ease of presentation, the projects are referred to by their first-
246 listed author and PubMed Unique Identifier (PMID). The details of each project are
247 summarized in Appendix 1 and Figure 1B, including the hospital name, city, and nation, as
248 well as the sample type, the MS method, the sample preparation method, and the PMID.

249
250 Of the 1,794 patients with gender and age information, 60.4% were male and the median age
251 was 49.1 years with a standard deviation of 17.12. Patients were categorized into seven
252 disease subgroups. A total of 1083 COVID-19 patients had non-severe disease, while 629 had
253 severe symptoms. Control cases, including healthy or non-COVID-19 patients, accounted for
254 19% and 12.5% of all cases, respectively. More than 80% of the samples were derived from
255 blood: 50.4% from plasma and 30.3% from sera. Besides blood samples, urine samples
256 constituted 9.6% and FFPE tissue 4.9% of all samples. As blood samples contain many high-
257 abundance proteins that may interfere with the identification of low abundant ones, some
258 studies performed additional depletion procedures on plasma or sera samples⁵⁶. Specifically,
259 4.2% of the plasma and 28.9% of the serum samples were depleted of the highly abundant
260 proteins. Regarding the mass spectrometry acquisition strategies used by the various studies,
261 label-free quantification methods, including DDA (13.5%), DIA (7%), MRM (0.3%),
262 scanning SWATH (2.5%), and SWATH (27.3%), were used for more than half of the
263 samples. Otherwise, the Olink kit (27.3%) or TMT multiplexing methods (19.2%) were used
264 (Table 1).

265
266 We next describe the analyses performed on the collected data and the results found.
267 Specifically, after general data evaluations, we performed protein, pathway, and integrative
268 analyses. We then demonstrate one of the possible use cases for the COVIDpro database.

269
270 To gain an overview of the various datasets, we first report the number of proteins identified
271 by each study with the mass spectrometry's missed detecting ratios. Although more than
272 14,403 proteins were measure by mass spectrometry across all projects, the largest proportion
273 of proteins were identified in non-sera and non-plasma datasets. More than ten thousand
274 proteins were detected in FFPE samples, while nasopharynx swabs accounted for over six
275 thousand proteins, urine for about three thousand proteins, and several hundreds of proteins
276 were measured in most sera and plasma samples. The number of proteins identified varies
277 between different clinical specimens (Figure 2A). The number of patients and their disease
278 subgroups are shown in Figure 2B. Most individual datasets described a few dozens to over a
279 hundred patients; the only exception was a study that profiled 384 patients, which had high
280 missing value rates.

281
282 Next, to perform functional analyses, we focused on 66 proteins identified in at least 70% of
283 the studies. Using a Gene Ontology (GO) analysis, we found that most of the identified
284 proteins were involved in the immune response and the activation of the complement system
285 (Figure 2C), which is consistent with previous findings that these proteins were more
286 involved in the regulation of COVID-19 severity⁹. We then further evaluated the most
287 frequently differentially expressed proteins. The most frequently appearing protein is the
288 lipopolysaccharide binding protein (LBP) which binds to lipopolysaccharide (LPS). The
289 latter has been reported to bind to SARS-CoV-2 S protein⁵⁷. LBP is known to increase in the
290 presence of bacterial infections and is a marker of sepsis⁵⁸⁻⁶⁰. It has been suggested that in

291 COVID-19 patients this LBP increase is caused by dysfunction of the gut-blood barrier that
292 leads to increased microbial translocation^{61,62}.

293

294 We then compared the expression of LBP across all the studies where it was detected. The
295 level of LBP increased significantly with the severity of disease, from healthy to non-severe
296 and severe groups, when sera and plasma samples were analyzed. By contrast, we observed
297 different LBP dynamics in urine, EV, colostrum, and cerebrospinal fluid samples (Figure 3A).
298 In COVID-19 autopsies, LBP was seen to have significantly decreased in the kidneys and
299 lungs (Figure 3B). Also, LBP showed slightly different expression dynamics in COVID-19
300 patients with prolonged RNA shedding (Figure 3C). Furthermore, the level of IL-6 also
301 positively correlated with the level of LBP (Figure 3D); IL-6 is known to be involved in both
302 fever and inflammation responses^{63,64}. The expression of IL-6 decreased in plasma during
303 convalescence (Figure 3E). Finally, in extracellular vesicle samples, LBP increased and then
304 decreased around the third week (Figure 3F). As elevated levels of LBP have also been
305 observed in infections and inflammatory diseases, this protein could be an indicator for the
306 severity progression of COVID-19.

307

308 Next, we analyzed and compared the urine proteomes of non-severe and healthy patients
309 from the Bi_2 dataset using the Student's *t*-test. We found that 59 and 839 proteins were up-
310 and down-regulated, respectively, in severe patients (Figure 4A). Using GO (Figure 4B) and
311 KEGG enrichment analyses (Figure 4C), we discovered that a large proportion of the up-
312 regulated proteins were involved in the central carbon cycles, while the down-regulated ones
313 were associated with binding and adhesion proteins. Empowered by *cyjshiny*⁵⁵ package and
314 KEGG pathway interactions taken from Pathway Commons version 12⁶⁵, which contains 79
315 common metabolic pathways, we identified 74 pathways containing these dysregulated
316 proteins. Six pathways having higher number of differentially changed proteins are shown in
317 Figure 4D. The down-regulated proteins were illustrated in the metabolism of the amino acids
318 while most up-regulated proteins were involved in the TCA cycles (Figure 4D). Compared
319 with the non-severe patients, many proteins involved in glycolysis and gluconeogenesis were
320 down-regulated in the urine samples of the severe cases; however, only a few proteins
321 involved in glycolysis and gluconeogenesis were dysregulated in the blood samples (Figure 4E).

322

323 COVIDpro's datasets can be used to explore and validate diagnostic biomarkers of COVID-
324 19. As a proof of principle, we generated a machine learning model for classifying COVID-
325 19 severity (severe vs. non-severe) based on specific proteins. First, using the tools provided
326 in our server, we identified the differentially expressed proteins between severe and non-
327 severe patients across all the studies that included these two categories (Figure 5A). We thus
328 focused on 51 differentially expressed proteins that appeared in at least five studies. Next, we
329 built a preliminary random forest model to classify COVID-19 severity using the Shen_1
330 dataset as the training set (Figure 5B). The top nine proteins were selected: SAA1,
331 SERPINA1, angiotensinogen (AGT), C9, LRG1, HBP2, SERPINA3, HRG, and HP (Figure
332 5C). These nine proteins were used to build a random forest-based classifier, which correctly
333 classified all COVID-19 cases from the Shen_1 dataset. Our classifier was then further
334 validated using five independent datasets, achieving a mean area under the curve (AUC) of
335 0.87 and a mean accuracy (ACC) of 0.79 (Figure 5D). Many of the selected proteins,
336 including the acute phase proteins SAA1 as well as the complement activation protein C9,
337 have been associated with severe patients⁶⁶. In addition, the serine protease inhibitor
338 SERPINA1/3 has been reported to inhibit the viral spike protein TRMPRSS2⁶⁷. AGT was
339 also a selected model feature. The enzymatic product of AGT is the precursor of angiotensin
340 II, which is the substrate of the host protein angiotensin-converting enzyme (ACE) homolog-

341 2 (ACE2). As a consequence, severe diseased COVID-19 patients have exhibited an elevated
342 expression of AGT⁶⁸. Of the genes we identified as part of our model, HABP2 has been
343 studied less thoroughly in connection with COVID-19, and our work suggests it warrants
344 further study. HABP2 plays a role in blood coagulation and may be involved in the
345 abnormalities of coagulation seen in COVID-19 patients^{69,70}.

346

347 **Discussion**

348 In this study, we generated a large public database, COVIDpro, including the most relevant
349 published proteomics datasets of COVID-19 patients. We also showed the results of a set of
350 analyses we performed using the toolkits available in COVIDpro. The COVIDpro database
351 covered the published proteomics data of COVID-19 patients till May 2022, containing 3077
352 patient cases, 5434 samples from 19 of sample types, and 14,403 proteins profiled. This data
353 resource allows performing meta-analyses of protein regulations across multiple clinical
354 specimens of COVID-19 patients from eleven nations. For each protein from the 14,403
355 proteins included in COVIDpro, we developed a user-friendly interface for browsing its
356 expression and pathway involvement across multiple datasets. This resource could be used to
357 support biomarker and therapeutic discoveries for COVID-19. As a showcase, we used
358 COVIDpro to identify biomarkers of COVID-19 severity and perform *in silico* validation
359 experiments. To the best of our knowledge, this is the most comprehensive COVID-19
360 protein expression repository.

361

362 We included a module to search for the latest relevant literature and another to append new
363 datasets to this database resource, allowing its timely update. The sever will be maintained
364 every quarter in the coming few years. The collected proteomic datasets were downloadable
365 as readable text tables or in an R object RDS format, allowing other researchers to re-analyze
366 the data for new discoveries. For example, identifications of clusters of proteins that go
367 beyond the severity of the disease; dysregulated proteins in different ages, genders and
368 geographical locations; specific patterns in the immune response for vaccine development.

369

370 Our data-driven study was different from the hypothesis-driven research, where more
371 combinations of results could be shown depending the questions to address using our online
372 database application. Here we only show one typical result and its interpretation due to the
373 space limitation. In addition, our study is phenomenological by nature for the observance of
374 the measured data, molecular functional validation cannot be surrogated to confirm the
375 dysregulated proteins as therapeutic targets or potential biomarkers for diagnostic prediction.

376

377 Constructed with an R shiny framework, the COVIDpro analysis pipeline works as a cross-
378 platform browser application that does not require any software installation. The R shiny
379 framework integrates well with JavaScript and Cascading Style Sheets (CSS), allowing
380 customized analysis modules to be generated. Our easy-to-access application allows users to
381 explore COVID-19 proteomics datasets and validate their hypotheses. This COVID-19pro
382 database may be a useful resource for navigating dysregulated proteins in various clinical
383 specimens from patients with COVID-19.

384 **References**

- 385 1 Walensky, R. P., Walke, H. T. & Fauci, A. S. SARS-CoV-2 Variants of Concern in
386 the United States-Challenges and Opportunities. *JAMA* **325**, 1037-1038,
387 doi:10.1001/jama.2021.2294 (2021).
- 388 2 Dong, E., Du, H. & Gardner, L. An interactive web-based dashboard to track COVID-
389 19 in real time. *Lancet Infect Dis* **20**, 533-534, doi:10.1016/S1473-3099(20)30120-1
390 (2020).
- 391 3 Iacopetta, D. *et al.* COVID-19 at a Glance: An Up-to-Date Overview on Variants,
392 Drug Design and Therapies. *Viruses* **14**, doi:10.3390/v14030573 (2022).
- 393 4 Robinson, P. C. *et al.* COVID-19 therapeutics: Challenges and directions for the
394 future. *Proc Natl Acad Sci U S A* **119**, e2119893119, doi:10.1073/pnas.2119893119
395 (2022).
- 396 5 Jin, Z. *et al.* Structure of M(pro) from SARS-CoV-2 and discovery of its inhibitors.
397 *Nature* **582**, 289-293, doi:10.1038/s41586-020-2223-y (2020).
- 398 6 Gao, Y. *et al.* Structure of the RNA-dependent RNA polymerase from COVID-19
399 virus. *Science* **368**, 779-782, doi:10.1126/science.abb7498 (2020).
- 400 7 Caruso, F. P., Scala, G., Cerulo, L. & Ceccarelli, M. A review of COVID-19
401 biomarkers and drug targets: resources and tools. *Brief Bioinform* **22**, 701-713,
402 doi:10.1093/bib/bbaa328 (2021).
- 403 8 Xiao, Q. *et al.* High-throughput proteomics and AI for cancer biomarker discovery.
404 *Adv Drug Deliv Rev* **176**, 113844, doi:10.1016/j.addr.2021.113844 (2021).
- 405 9 Shen, B. *et al.* Proteomic and Metabolomic Characterization of COVID-19 Patient
406 Sera. *Cell* **182**, 59-72 e15, doi:10.1016/j.cell.2020.05.032 (2020).
- 407 10 Zhu, Y., Aebersold, R., Mann, M. & Guo, T. SnapShot: Clinical proteomics. *Cell* **184**,
408 4840-4840 e4841, doi:10.1016/j.cell.2021.08.015 (2021).
- 409 11 D'Alessandro, A. *et al.* Serum Proteomics in COVID-19 Patients: Altered Coagulation
410 and Complement Status as a Function of IL-6 Level. *J Proteome Res* **19**, 4417-4427,
411 doi:10.1021/acs.jproteome.0c00365 (2020).
- 412 12 Demichev, V. *et al.* A time-resolved proteomic and prognostic map of COVID-19.
413 *Cell Syst*, doi:10.1016/j.cels.2021.05.005 (2021).
- 414 13 Gisby, J. *et al.* Longitudinal proteomic profiling of dialysis patients with COVID-19
415 reveals markers of severity and predictors of death. *Elife* **10**, doi:10.7554/eLife.64827
416 (2021).
- 417 14 Lee, J. S. *et al.* Longitudinal proteomic profiling provides insights into host response
418 and proteome dynamics in COVID-19 progression. *Proteomics* **21**, e2000278,
419 doi:10.1002/pmic.202000278 (2021).
- 420 15 Leng, L. *et al.* Sera proteomic features of active and recovered COVID-19 patients:
421 potential diagnostic and prognostic biomarkers. *Signal Transduct Target Ther* **6**, 216,
422 doi:10.1038/s41392-021-00612-5 (2021).
- 423 16 Messner, C. B. *et al.* Ultra-High-Throughput Clinical Proteomics Reveals Classifiers
424 of COVID-19 Infection. *Cell Syst* **11**, 11-24 e14, doi:10.1016/j.cels.2020.05.012
425 (2020).
- 426 17 Villar, M. *et al.* Characterization by Quantitative Serum Proteomics of Immune-
427 Related Prognostic Biomarkers for COVID-19 Symptomatology. *Front Immunol* **12**,
428 730710, doi:10.3389/fimmu.2021.730710 (2021).
- 429 18 Völlmy, F. *et al.* A serum proteome signature to predict mortality in severe COVID-
430 19 patients. *Life Sci Alliance* **4**, doi:10.26508/lsa.202101099 (2021).
- 431 19 Wu, P. *et al.* The trans-omics landscape of COVID-19. *Nat Commun* **12**, 4543,
432 doi:10.1038/s41467-021-24482-1 (2021).

- 433 20 Yang, J. *et al.* Proteomics and metabolomics analyses of Covid-19 complications in
434 patients with pulmonary fibrosis. *Sci Rep* **11**, 14601, doi:10.1038/s41598-021-94256-
435 8 (2021).
- 436 21 Wang, H. *et al.* Next-Generation Sequencing and Proteomics of Cerebrospinal Fluid
437 From COVID-19 Patients With Neurological Manifestations. *Front Immunol* **12**,
438 782731, doi:10.3389/fimmu.2021.782731 (2021).
- 439 22 Filbin, M. R. *et al.* Longitudinal proteomic analysis of severe COVID-19 reveals
440 survival-associated signatures, tissue-specific cell death, and cell-cell interactions.
441 *Cell Rep Med* **2**, 100287, doi:10.1016/j.xcrm.2021.100287 (2021).
- 442 23 Fisher, J. *et al.* Proteome Profiling of Recombinant DNase Therapy in Reducing
443 NETs and Aiding Recovery in COVID-19 Patients. *Mol Cell Proteomics* **20**, 100113,
444 doi:10.1016/j.mcpro.2021.100113 (2021).
- 445 24 Messner, C. B. *et al.* Ultra-fast proteomics with Scanning SWATH. *Nat Biotechnol* **39**,
446 846-854, doi:10.1038/s41587-021-00860-4 (2021).
- 447 25 Park, J. *et al.* In-depth blood proteome profiling analysis revealed distinct functional
448 characteristics of plasma proteins between severe and non-severe COVID-19 patients.
449 *Sci Rep* **10**, 22418, doi:10.1038/s41598-020-80120-8 (2020).
- 450 26 Patel, H. *et al.* Proteomic blood profiling in mild, severe and critical COVID-19
451 patients. *Sci Rep* **11**, 6357, doi:10.1038/s41598-021-85877-0 (2021).
- 452 27 Shu, T. *et al.* Plasma Proteomics Identify Biomarkers and Pathogenesis of COVID-19.
453 *Immunity* **53**, 1108-1122 e1105, doi:10.1016/j.immuni.2020.10.008 (2020).
- 454 28 Suvarna, K. *et al.* Proteomics and Machine Learning Approaches Reveal a Set of
455 Prognostic Markers for COVID-19 Severity With Drug Repurposing Potential. *Front*
456 *Physiol* **12**, 652799, doi:10.3389/fphys.2021.652799 (2021).
- 457 29 Suvarna, K. *et al.* A Multi-omics Longitudinal Study Reveals Alteration of the
458 Leukocyte Activation Pathway in COVID-19 Patients. *J Proteome Res* **20**, 4667-4680,
459 doi:10.1021/acs.jproteome.1c00215 (2021).
- 460 30 Wang, C. *et al.* Multi-omic profiling of plasma reveals molecular alterations in
461 children with COVID-19. *Theranostics* **11**, 8008-8026, doi:10.7150/thno.61832
462 (2021).
- 463 31 Zhong, W. *et al.* Next generation plasma proteome profiling of COVID-19 patients
464 with mild to moderate symptoms. *EBioMedicine* **74**, 103723,
465 doi:10.1016/j.ebiom.2021.103723 (2021).
- 466 32 Al-Nesf, M. A. Y. *et al.* Prognostic tools and candidate drugs based on plasma
467 proteomics of patients with severe COVID-19 complications. *Nat Commun* **13**, 946,
468 doi:10.1038/s41467-022-28639-4 (2022).
- 469 33 Carapito, R. *et al.* Identification of driver genes for critical forms of COVID-19 in a
470 deeply phenotyped young patient cohort. *Sci Transl Med*, eabj7521,
471 doi:10.1126/scitranslmed.abj7521 (2021).
- 472 34 Li, J. *et al.* Virus-Host Interactome and Proteomic Survey Reveal Potential Virulence
473 Factors Influencing SARS-CoV-2 Pathogenesis. *Med (N Y)* **2**, 99-112 e117,
474 doi:10.1016/j.medj.2020.07.002 (2021).
- 475 35 Nie, X. *et al.* Multi-organ proteomic landscape of COVID-19 autopsies. *Cell* **184**,
476 775-791 e714, doi:10.1016/j.cell.2021.01.004 (2021).
- 477 36 Wanner, N. *et al.* Molecular consequences of SARS-CoV-2 liver tropism. *Nat Metab*
478 **4**, 310-319, doi:10.1038/s42255-022-00552-6 (2022).
- 479 37 Bi. in revision. (2021).
- 480 38 Chavan, S. *et al.* Mass Spectrometric Analysis of Urine from COVID-19 Patients for
481 Detection of SARS-CoV-2 Viral Antigen and to Study Host Response. *J Proteome*
482 *Res* **20**, 3404-3413, doi:10.1021/acs.jproteome.1c00391 (2021).

- 483 39 Li, Y. *et al.* Urine proteome of COVID-19 patients. *Urine (Amst)* **2**, 1-8,
484 doi:10.1016/j.urine.2021.02.001 (2020).
- 485 40 Tian, W. *et al.* Immune suppression in the early stage of COVID-19 disease. *Nat*
486 *Commun* **11**, 5859, doi:10.1038/s41467-020-19706-9 (2020).
- 487 41 Liu, Y. *et al.* A urinary proteomic landscape of COVID-19 progression identifies
488 signaling pathways and therapeutic options. *Sci China Life Sci*, doi:10.1007/s11427-
489 021-2070-y (2022).
- 490 42 He, F. *et al.* Fecal multi-omics analysis reveals diverse molecular alterations of gut
491 ecosystem in COVID-19 patients. *Anal Chim Acta* **1180**, 338881,
492 doi:10.1016/j.aca.2021.338881 (2021).
- 493 43 Lam, S. M. *et al.* A multi-omics investigation of the composition and function of
494 extracellular vesicles along the temporal trajectory of COVID-19. *Nat Metab* **3**, 909-
495 922, doi:10.1038/s42255-021-00425-4 (2021).
- 496 44 Pesce, E. *et al.* Exosomes Recovered From the Plasma of COVID-19 Patients Expose
497 SARS-CoV-2 Spike-Derived Fragments and Contribute to the Adaptive Immune
498 Response. *Front Immunol* **12**, 785941, doi:10.3389/fimmu.2021.785941 (2021).
- 499 45 Ghosh, S. *et al.* Semen Proteomics of COVID-19 Convalescent Men Reveals
500 Disruption of Key Biological Pathways Relevant to Male Reproductive Function.
501 *ACS Omega* **7**, 8601-8612, doi:10.1021/acsomega.1c06551 (2022).
- 502 46 Zeng, H. L. *et al.* Proteomic characteristics of bronchoalveolar lavage fluid in critical
503 COVID-19 patients. *Febs j* **288**, 5190-5200, doi:10.1111/febs.15609 (2021).
- 504 47 Zhao, Y. *et al.* Omics study reveals abnormal alterations of breastmilk proteins and
505 metabolites in puerperant women with COVID-19. *Signal Transduct Target Ther* **5**,
506 247, doi:10.1038/s41392-020-00362-w (2020).
- 507 48 Vanderboom, P. M. *et al.* Proteomic Signature of Host Response to SARS-CoV-2
508 Infection in the Nasopharynx. *Mol Cell Proteomics* **20**, 100134,
509 doi:10.1016/j.mcpro.2021.100134 (2021).
- 510 49 Qi, C. *et al.* SCovid: single-cell atlases for exposing molecular characteristics of
511 COVID-19 across 10 human tissues. *Nucleic Acids Res* **50**, D867-D874,
512 doi:10.1093/nar/gkab881 (2022).
- 513 50 Zhang, W. *et al.* COVID19db: a comprehensive database platform to discover
514 potential drugs and targets of COVID-19 at whole transcriptomic scale. *Nucleic Acids*
515 *Res* **50**, D747-D757, doi:10.1093/nar/gkab850 (2022).
- 516 51 Harrison, P. W. *et al.* The COVID-19 Data Portal: accelerating SARS-CoV-2 and
517 COVID-19 research through rapid open access data sharing. *Nucleic Acids Res* **49**,
518 W619-W623, doi:10.1093/nar/gkab417 (2021).
- 519 52 De Silva, N. H. *et al.* The Ensembl COVID-19 resource: ongoing integration of public
520 SARS-CoV-2 data. *Nucleic Acids Res* **50**, D765-D770, doi:10.1093/nar/gkab889
521 (2022).
- 522 53 Carlson, M. org.Hs.eg.db: Genome wide annotation for Human. *R package version*
523 *3.12.0* (2020).
- 524 54 Wu, T. *et al.* clusterProfiler 4.0: A universal enrichment tool for interpreting omics
525 data. *The Innovation* **2**, doi:10.1016/j.xinn.2021.100141 (2021).
- 526 55 Luna, A. cytoscape/r-cytoscape.js: r-cytoscape.js 0.0.7 *Zenodo* (2018).
- 527 56 Cao, X. *et al.* Evaluation of Spin Columns for Human Plasma Depletion to Facilitate
528 MS-Based Proteomics Analysis of Plasma. *J Proteome Res* **20**, 4610-4620,
529 doi:10.1021/acs.jproteome.1c00378 (2021).
- 530 57 Petruk, G. *et al.* SARS-CoV-2 spike protein binds to bacterial lipopolysaccharide and
531 boosts proinflammatory activity. *J Mol Cell Biol* **12**, 916-932,
532 doi:10.1093/jmcb/mjaa067 (2020).

- 533 58 Schumann, R. R. Old and new findings on lipopolysaccharide-binding protein: a
534 soluble pattern-recognition molecule. *Biochem Soc Trans* **39**, 989-993,
535 doi:10.1042/BST0390989 (2011).
- 536 59 Opal, S. M. *et al.* Relationship between plasma levels of lipopolysaccharide (LPS)
537 and LPS-binding protein in patients with severe sepsis and septic shock. *J Infect Dis*
538 **180**, 1584-1589, doi:10.1086/315093 (1999).
- 539 60 Blairon, L., Wittebole, X. & Laterre, P. F. Lipopolysaccharide-binding protein serum
540 levels in patients with severe sepsis due to gram-positive and fungal infections. *J*
541 *Infect Dis* **187**, 287-291, doi:10.1086/346046 (2003).
- 542 61 Samsudin, F. *et al.* SARS-CoV-2 spike protein as a bacterial lipopolysaccharide
543 delivery system in an overzealous inflammatory cascade. *bioRxiv*,
544 2021.2010.2029.466401, doi:10.1101/2021.10.29.466401 (2021).
- 545 62 Assimakopoulos, S. F. *et al.* SARS CoV-2-Induced Viral Sepsis: The Role of Gut
546 Barrier Dysfunction. *Microorganisms* **10**, doi:10.3390/microorganisms10051050
547 (2022).
- 548 63 Tanaka, T., Narazaki, M. & Kishimoto, T. IL-6 in inflammation, immunity, and
549 disease. *Cold Spring Harb Perspect Biol* **6**, a016295,
550 doi:10.1101/cshperspect.a016295 (2014).
- 551 64 Kaiser, L., Fritz, R. S., Straus, S. E., Gubareva, L. & Hayden, F. G. Symptom
552 pathogenesis during acute influenza: interleukin-6 and other cytokine responses. *J*
553 *Med Virol* **64**, 262-268, doi:10.1002/jmv.1045 (2001).
- 554 65 Rodchenkov, I. *et al.* Pathway Commons 2019 Update: integration, analysis and
555 exploration of pathway data. *Nucleic Acids Res* **48**, D489-D497,
556 doi:10.1093/nar/gkz946 (2020).
- 557 66 Wang, L. *et al.* CRP, SAA, LDH, and DD predict poor prognosis of coronavirus
558 disease (COVID-19): a meta-analysis from 7739 patients. *Scand J Clin Lab Invest* **81**,
559 679-686, doi:10.1080/00365513.2021.2000635 (2021).
- 560 67 Hoffmann, M. *et al.* SARS-CoV-2 Cell Entry Depends on ACE2 and TMPRSS2 and
561 Is Blocked by a Clinically Proven Protease Inhibitor. *Cell* **181**, 271-+,
562 doi:10.1016/j.cell.2020.02.052 (2020).
- 563 68 Aksoy, H., Karadag, A. S. & Wollina, U. Angiotensin II receptors: Impact for
564 COVID-19 severity. *Dermatol Ther* **33**, e13989, doi:10.1111/dth.13989 (2020).
- 565 69 Teimury, A., Khameneh, M. T. & Khaledi, E. M. Major coagulation disorders and
566 parameters in COVID-19 patients. *Eur J Med Res* **27**, 25, doi:10.1186/s40001-022-
567 00655-6 (2022).
- 568 70 Li, W. *et al.* SARS-CoV-2 RNA elements share human sequence identity and
569 upregulate hyaluronan via NamiRNA-enhancer network. *EBioMedicine* **76**, 103861,
570 doi:10.1016/j.ebiom.2022.103861 (2022).

571

572

573 **Figure legends**

574

575 **Figure 1 Study design.** (A) Selection of a set of COVID-19 proteomics datasets. (B) List of
576 the COVID-19 studies selected for our database.

577

578 **Figure 2 Protein expression in the COVID-19 datasets selected for COVIDpro.** (A)
579 Upper panel: the number of proteins in each dataset; lower panel: the 76 most frequently
580 characterized proteins in the database. (B) Number of patients involved in each study. (C) GO
581 enrichment of the biological processes involving the 76 most frequently identified proteins.

582

583 **Figure 3 Meta-analysis of LBP expression.** (A) Expression of LBP in non-longitudinal
584 studies. (B) Expression of LBP in seven FFPE tissues. (C) Expression of LBP in a study
585 including cases with either a long (LC) or a short course (SC) of the disease. (D) Expression
586 of LBP in a study where samples were grouped according to IL-6 expression. (E) Expression
587 of LBP in two longitudinal plasma studies. (F) Expression of LBP in longitudinal EV
588 samples.

589

590 **Figure 4 Pathway analysis of the differentially expressed proteins of COVID-19**
591 **patients.** (A) Volcano plots for differentially expressed proteins (DEPs) in non-severe vs.
592 healthy cases from the Bi_2 dataset. (B) GO enrichment results of the up- and down-
593 regulated DEPs. (C) KEGG enrichment results of the up- and down-regulated DEPs. (D)
594 Selected pathways from the Bi_2 dataset involving dysregulated proteins. Red (up) and blue
595 (down) indicate the direction of the regulation. (E) Differentially changed proteins in
596 glycolysis and gluconeogenesis for severe and non-severe cases.

597

598 **Figure 5 Differentially expressed proteins between severe and non-severe patients and**
599 **machine learning modeling.** (A) Volcano plots of the differentially expressed proteins in
600 non-severe vs. severe patients across all the datasets containing these patient groups. (B) The
601 51 dysregulated proteins that appeared in at least five projects. (C) The nine features with the
602 highest mean decrease Gini from the random forest model. (D) Performance of random forest
603 classifier for training and independent validation cohorts, including Receiver operation
604 curves (ROCs), Area under curves (AUCs), and accuracies (ACCs).

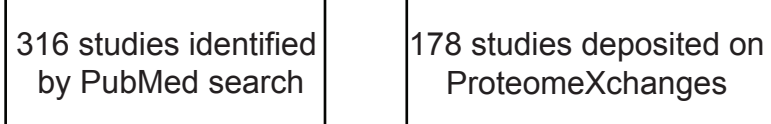
605 **Table 1 Baseline characteristics of the patient included**

Gender	
Female	745/1847(40.3%)
Male	1102/1847(59.7%)
Age	
	49.1(17.12)(n=1794)
Disease subgroup	
Healthy	586/3077(19%)
Non COVID-19	385/3077(12.5%)
COVID-19 (non-severe)	1083/3077(35.2%)
COVID-19 (severe)	629/3077(20.4%)
COVID-19 (fatal)	85/3077(2.8%)
COVID-19 (critical)	212/3077(6.9%)
Non-pulmonary fibrosis	6/3077(0.2%)
Pulmonary fibrosis	21/3077(0.7%)
COVID-19 (non-critical)	21/3077(0.7%)
Control IL-6	16/3077(0.5%)
Low IL-6	18/3077(0.6%)
Medium IL-6	5/3077(0.2%)
High IL-6	10/3077(0.3%)
Clinical sample type	
Bronchoalveolar lavage fluid	9/5434(0.2%)
Cerebrospinal fluid	8/5434(0.1%)
Colostrum	6/5434(0.1%)
Extracellular vesicle	23/5434(0.4%)
Fecal	72/5434(1.3%)
Heart FFPE	38/5434(0.7%)
Kidney FFPE	61/5434(1.1%)
Liver FFPE	52/5434(1%)
Lung FFPE	37/5434(0.7%)
Nasopharynx swabs	16/5434(0.3%)
PBMC	103/5434(1.9%)
Plasma	2737/5434(50.4%)
Semen	27/5434(0.5%)
Sera	1645/5434(30.3%)
Spleen FFPE	32/5434(0.6%)
Sputa	13/5434(0.2%)
Testis FFPE	15/5434(0.3%)
Thyroid FFPE	29/5434(0.5%)
Urine	511/5434(9.4%)
Sample preparation method	
Acetone precipitation	149/5434(2.7%)
Breast pump	6/5434(0.1%)
DTT	44/5434(0.8%)

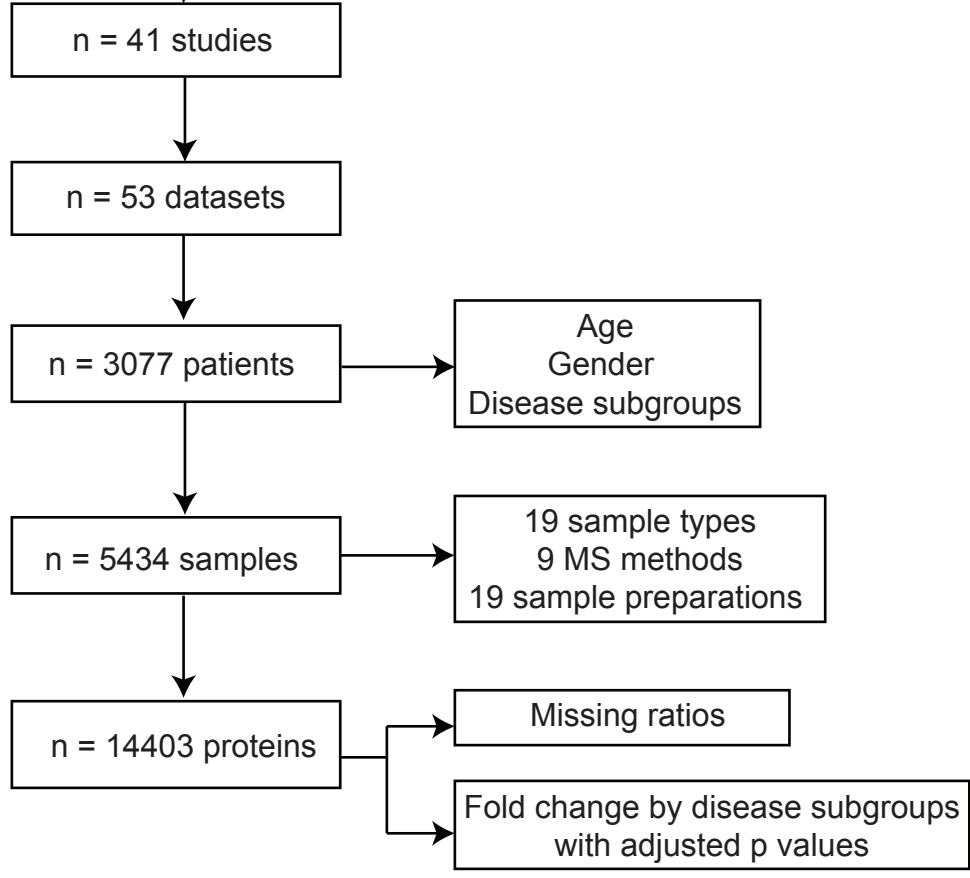
Ethanol precipitation	27/5434(0.5%)
Fecal boiling	72/5434(1.3%)
filter 3kDa	10/5434(0.2%)
Immune affinity purification	11/5434(0.2%)
iST kit	77/5434(1.4%)
Methanol precipitation	16/5434(0.3%)
PCT	248/5434(4.6%)
Plasma depletion	115/5434(2.1%)
Plasma non-depletion	2535/5434(46.7%)
RapiGest	13/5434(0.2%)
RBC removal	8/5434(0.1%)
Serum depletion	476/5434(8.8%)
Serum non-depletion	1169/5434(21.5%)
Sonication	16/5434(0.3%)
Ultracentrifugation	329/5434(6.1%)
Unknown	113/5434(2.1%)
<hr/> MS methods	
DDA	732/5434(13.5%)
DIA	381/5434(7%)
ELISA	11/5434(0.2%)
MRM	19/5434(0.3%)
Olink	1491/5434(27.4%)
Scanning SWATH	134/5434(2.5%)
SWATH	1485/5434(27.3%)
TMT	1044/5434(19.2%)
Unknown	137/5434(2.5%)

606

A

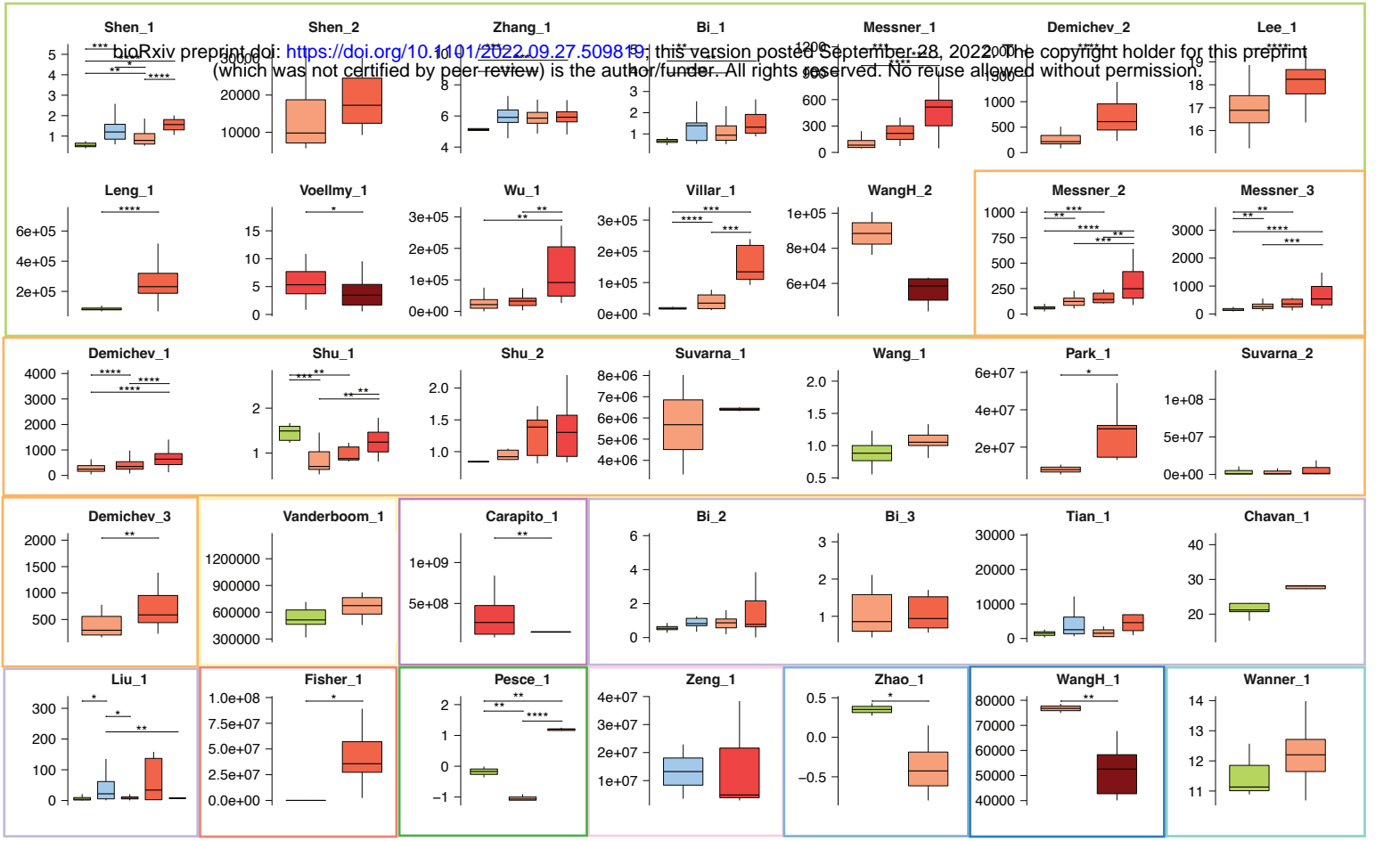
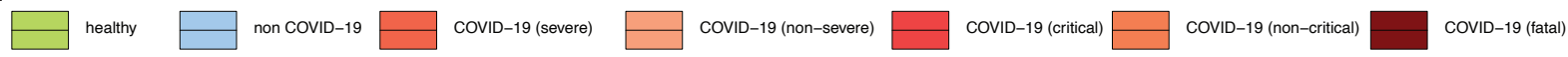


bioRxiv preprint doi: <https://doi.org/10.1101/2022.09.27.509819>; this version posted September 28, 2022. The copyright holder for this preprint (which was not certified by peer review) is the author/funder. All rights reserved. No reuse allowed without permission.



B

Hospital	Project	Disease subgroup	MS method	Sample type	Sample preparation
Charite Universitaetsmedizin, Berlin, Germany	Ai-Nesf et al.	healthy	DDA	Bronchoalveolar lavage fluid	Acetone precipitation
Columbia Irving, New York, United States	Alessandro et al.	non COVID-19	DIA	Cerebrospinal fluid	Breast pump
Ditan, Beijing, China	Bi et al.	COVID-19 (non-severe)	ELISA	Colostr	Dithiothreitol
Enze Hospital, Taizhou, China	Carapito et al.	COVID-19 (severe)	MRM	Extracellular vesicle	Ethanol precipitation
First Hospital, Wenzhou, China	Chavan et al.	COVID-19 (non-critical)	Olink	Fecal	Fecal boiling
Guangzhou Eighth People's Hospital, Guangzhou, China	Demichev et al.	COVID-19 (critical)	Scanning SWATH	FFPE lung	Filter 3kDa
Hamad Medical Corporation, Doha, Qatar	Fisher et al.	COVID-19 (fatal)	SWATH	FFPE spleen	Immune affinity purification
Hospital Civil, Strasbourg, France	Filbin et al.	non pulmonary fibrosis	TMT	FFPE liver	iST
Hospital General Universitario, Ciudad Real, Spain	Ghosh et al.	pulmonary fibrosis	Unknown	FFPE heart	Methanol precipitation
Imperial, London, United Kingdom	Gisby et al.			FFPE kidney	PCT
Jaslak Hospital, Mumbai, India	He et al.			FFPE testis	Plasma depletion
Jinyintan, Wuhan, China	Ho et al.			FFPE thyroid	Plasma non-depletion
Kasturba Hospital, Mumbai, India	Lam et al.			Nasopharynx swabs	RapiGest
Landeskrankenhaus, Innsbruck, Austria	Lee et al.			PBMC	RBC removal
Massachusetts General Hospital, Boston, United States	Leng et al.			Plasma	Serum depletion
Mayo Clinic Hospital, Minnesota, United States	Li J. et al.			Semen	Serum non-depletion
National Medical Center, Seoul, China	Li Y. et al.			Sera	Sonication
Ospedale Maggiore Policlinico, Milan, Italy	Liu et al.			Sputa	Ultracentrifugation
Ospedale Maggiore Policlinico, Milan, Italy	Messner et al.			Urine	Unknown
People's Hospital, Nanning, China	Nie et al.				
PLA General, Beijing, China	Park et al.				
Sahlgrenska University Hospital, Gothenburg, Sweden					
Skane University Hospital, Lund, Sweden					
SPHCC, Shanghai, China					
Sun Yat-Sen, Guangzhou, China					
Tongji Hospital, Wuhan, China					
Umraniye, Istanbul, Turkey					
Union Hospital, Wuhan, China					
University Hospital, Ferrara, Italy					
University Medical Center, Hamburg, Germany					
Women, Guangzhou, China					
Wuhan Red-Cross Hospital, Wuhan, China					
Youan Hospital, Beijing, China					



↑ Intensity

